The endoplasmic reticulum–resident collagen chaperone Hsp47 interacts with and promotes the secretion of decorin, fibromodulin, and lumican

Received for publication, November 2, 2017, and in revised form, June 29, 2018 Published, Papers in Press, July 12, 2018, DOI 10.1074/jbc.RA117.000758

Yoshihiro Ishikawa[‡§], **Kristofer Rubin**[¶1], **Hans Peter Bächinger**[‡§], **and Sebastian Kalamajski**[¶2]

From the [‡]*Department of Biochemistry and Molecular Biology, Oregon Health and Science University, Portland, Oregon 97239, the* [§]*Research Department, Shriners Hospital for Children, Portland, Oregon 97239, and the* [¶]*Department for Medical Biochemistry and Microbiology, Uppsala University, Uppsala 75237, Sweden*

Edited by Amanda J. Fosang

The build-up of diversified and tissue-specific assemblies of extracellular matrix (ECM) proteins depends on secreted and cell surface–located molecular arrays that coordinate ECM proteins into discrete designs. The family of small leucine-rich proteins (SLRPs) associates with and dictates the structure of fibrillar collagens, which form the backbone of most ECM types. However, whether SLRPs form complexes with proteins other than collagens is unclear. Here, we demonstrate that heat shock protein 47 (Hsp47), a well-established endoplasmic reticulum–resident collagen chaperone, also binds the SLRPs decorin, lumican, and fibromodulin with affinities comparable with that in the Hsp47–type I collagen interaction. Furthermore, we show that a lack of Hsp47 inhibits the cellular secretion of decorin and lumican. Our results expand the understanding of the concerted molecular interactions that control the secretion and organization of a functional collagenous ECM.

Extracellular matrices (ECMs)[3] are to a large extent composed of collagens assembled into cross-linked fibrils. The build-up of the ECM requires cellular secretion from the rough endoplasmic reticulum (rER) using COPII vesicles and the trafficking of large amounts of collagens, ensured by special transport vesicles (1–3). Collagen fibrillogenesis commences already during intracellular transport and continues to assemble to fibril precursors in post-Golgi recesses following enzymatic processing of procollagen propeptides (4, 5). Besides this special toolkit of proteins required for proper collagen transport and processing, a large number of other molecules, including post-translational modifiers, enzymes, and chaperones, have been found in the rER (6–8).

Efficient procollagen secretion requires a collective action of several intracellular transport– and/or sorting–associated proteins, including TANGO1 (9, 10), cTAGE5 (11, 12), Sedlin (13), and Sec proteins (11, 14, 15). These proteins function at the ER exit sites to ensure efficient sorting into and enlarging of special transport vesicles, as COPII vesicles cannot carry the large procollagen cargo. Hsp47 plays an important role during this sorting stage and functions as an anchor molecule between TANGO1 and procollagens (16). Hsp47 is crucial during procollagen biosynthesis, because Hsp47 deficiency results in procollagen aggregating in the ER (17), and the deficiency also leads to embryonic lethality (18, 19). Missense mutations in the *SERPINH1* gene (which encodes Hsp47) cause osteogenesis imperfecta in humans and dogs (20, 21). Hsp47 was originally characterized as a collagen-specific molecular chaperone (22, 23); it has been shown, however, to interact with fibrillin-1 (16). Also, Hsp47 has recently been found to modulate the unfolded protein response (24).

Here, we wanted to explore whether small leucine-rich proteins (SLRPs) are involved in early collagen biosynthesis in the ER via complex formation with other intracellular collagen–associated proteins. SLRPs are already known to modulate the phenotype of collagen fibrils and their cross-linking in the extracellular space (25–28); thus, we hypothesized that their function might be required at the rER or ER exit sites for and during secretion of procollagen. Such a, yet unknown, mechanism would ensure a proper modulatory SLRP function during the early, intracellular stages of collagen fibrillogenesis (*i.e.* even before the deposition in extracellular space). In this report, we investigated whether the collagen-associated SLRPs decorin (29, 30), lumican (31, 32), and fibromodulin (33, 34) could interact with any intracellular collagen–associated proteins and, if so, what the consequences of these interactions might be.

Results

Decorin, fibromodulin, and lumican interact with Hsp47 in cell lysates

Far-Western blotting was used to find potential intracellular interactants of decorin, fibromodulin, and lumican. Cell lysate from a chondrocyte-like ATDC5 cell line was run on SDS-PAGE and transferred to a nitrocellulose membrane that was

This study was supported in part by Shriners Hospital for Children Grants 85100 and 85500 (to H. P. B.). The authors declare that they have no conflicts of interest with the contents of this article.

This article contains Figs. S1–S5.

[1] Supported by the Swedish Cancer Foundation.

[2] Supported by the Swedish Cancer Foundation, the Crafoord Foundation, the Åke Wiberg Foundation, and the Magnus Bergvall Foundation. To whom correspondence should be addressed. E-mail: sebastian.kalamajski@imbim.uu.se.

[3] The abbreviations used are: ECM, extracellular matrix; ER, endoplasmic reticulum; rER, rough endoplasmic reticulum; SLRP, small leucine-rich protein; SPR, surface plasmon resonance; SH3, Src homology 3; PLA, proximity ligation assay; RU, reference units; DMEM, Dulbecco's modified Eagle's medium; BisTris, 2-[bis(2-hydroxyethyl)amino]-2-(hydroxymethyl)propane-1,3-diol; DCN, decorin; FM, fibromodulin; LUM, lumican; HRP, horseradish peroxidase.

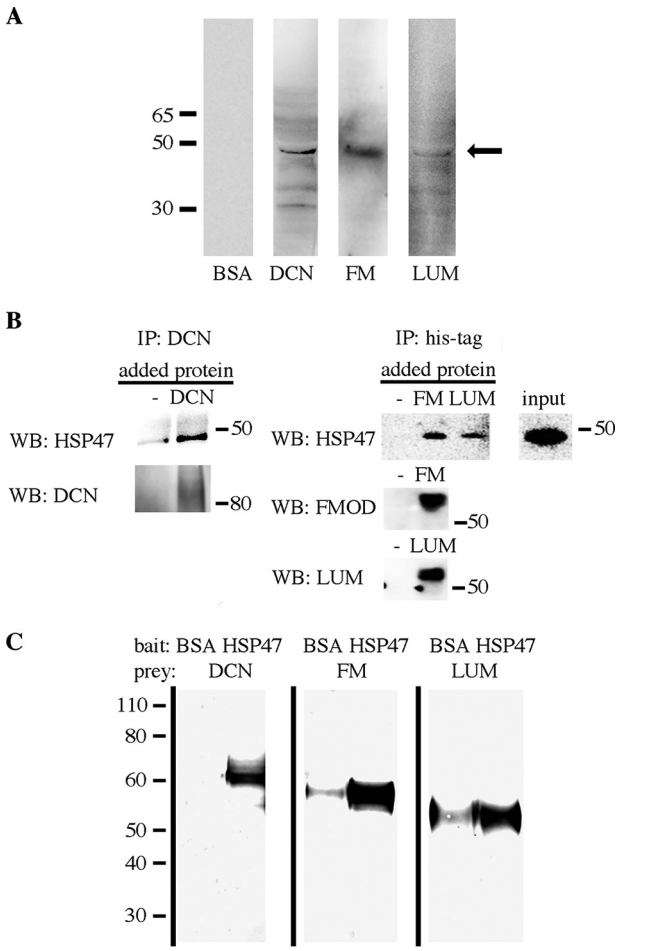

Figure 1. Discovery and validation of SLRP–Hsp47 interactions. *A*, far-Western blotting to detect potential intracellular SLRP interactants. Lysates of chondrocyte-like ATDC5 cells were run on SDS-PAGE, and the proteins were transferred onto a nitrocellulose membrane. Membrane strips were blocked with BSA and incubated with biotinylated proteins: BSA (negative control), decorin (DCN), fibromodulin (FM), or lumican (LUM). Binding was detected with streptavidin-HRP and peroxidase substrate. The *arrow* marks a presumed common interactant of DCN, FM, and LUM. The corresponding region was cut out from the SDS-polyacrylamide gel and analyzed by MS. *B*, co-immunoprecipitation assays to detect potential SLRP–Hsp47 interactions. Lysates from ATDC5 cells were used alone (−) or mixed with 1 μg of recombinant DCN, His-tagged FM, or His-tagged LUM. The lysates were incubated with decorin rabbit anti-serum (*IP*: *DCN*) or mouse anti-His antibodies (*IP*: *his-tag*) and with Protein A– or Protein G–Sepharose, respectively. Co-precipitated proteins were run on SDS-PAGE and immunoblotted for Hsp47 (*WB*: *HSP47*). The capture of SLRPs was validated with the corresponding antisera (*WB*: *DCN*, *FM*, *LUM*). *C*, pulldown assays to validate SLRP–Hsp47 interactions. Magnetic beads were coated with BSA or Hsp47 (bait) and incubated with biotinylated DCN, FM, or LUM (all prey). The beads were washed, and the eluates were run on SDS-PAGE. The binding was detected by blotting with streptavidin-HRP.

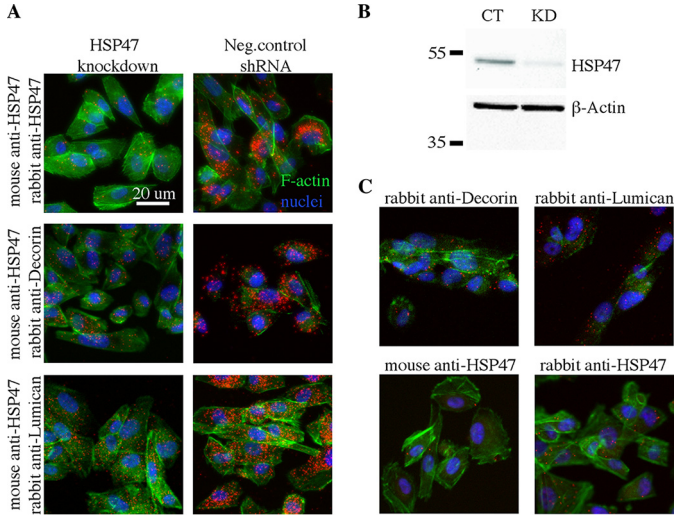

Figure 2. Proximity ligation assays for validation of intracellular SLRP–Hsp47 interactions. BJ human fibroblasts were transfected with shRNA against Hsp47 (*KD*) or with a universal negative control shRNA (*CT*). *A*, cells were seeded on glass slides, and PLA assays were performed using the indicated antibody combinations. The combination of the two different anti-Hsp47 antibodies was to validate the knockdown. The combinations of anti-Hsp47 and the respective SLRP anti-sera were used to detect Hsp47–SLRP interactions. Images are representative of two independent experiments. Interactions are indicated by *red fluorescence*, F-actin is shown in *green*, and nuclei are shown in *blue*. *B*, the Hsp47 knockdown efficiency was confirmed by immunoblotting cell lysates for Hsp47 with for β-actin as internal loading control. *C*, representative images of additional negative controls, where the cells were incubated with a combination of both secondary antibodies and only one respective primary antibody.

then incubated with biotinylated recombinant decorin, fibromodulin, or lumican. Although decorin, unlike fibromodulin and lumican, bound to several other proteins (possibly through its chondroitin/dermatan sulfate chains), all three SLRPs interacted with a protein around 48–50 kDa (Fig. 1*A*). The corresponding area on the SDS-polyacrylamide gel was analyzed by MS, where five peptides from Hsp47 were found (Fig. S1). Because Hsp47 is an ER-resident collagen chaperone, residing in the same subcellular compartment as the secreted SLRPs, Hsp47–SLRP interactions were validated with further experiments (below). Other proteins identified by MS were either nuclear or cytoskeletal proteins; they were not considered in further analyses.

To characterize the SLRP–Hsp47 interactions, co-immunoprecipitations were performed using cell lysates. As endogenous intracellular amounts of SLRPs were not abundant, exogenous purified recombinant decorin, fibromodulin, or lumican (the latter two His-tagged) were added to the cell lysate and immunoprecipitated using decorin antiserum or His tag antibodies. In these assays, Hsp47 precipitated together with all three SLRPs and did not precipitate in the absence of SLRPs (Fig. 1*B*). To validate our findings, further pulldown assays were also performed, where BSA or recombinant Hsp47 were coupled to magnetic beads, and then these beads were incubated with biotinylated recombinant decorin, fibromodulin, or lumican. In all cases, SLRPs were captured by Hsp47-coated beads but not by BSA-coated beads (Fig. 1*C*). These results indicate that Hsp47 could associate with the investigated SLRPs.

Proximity ligation assays show intracellular interaction between Hsp47 and decorin and lumican

To investigate whether the SLRP–Hsp47 interactions are present in intracellular compartments, we used proximity ligation assays using human BJ fibroblasts, mouse or rabbit anti-Hsp47, and rabbit anti-decorin or anti-lumican antibodies (Fig. 2). In two independent experiments, clear signals were detected in cells transfected with negative control shRNA, whereas low signals were detected in cells transfected with Hsp47 knockdown shRNA. This strongly suggests an association between Hsp47 and the two SLRPs. As Hsp47 is an ER-resident protein (22, 35), these data show that Hsp47 and the SLRPs occur in the

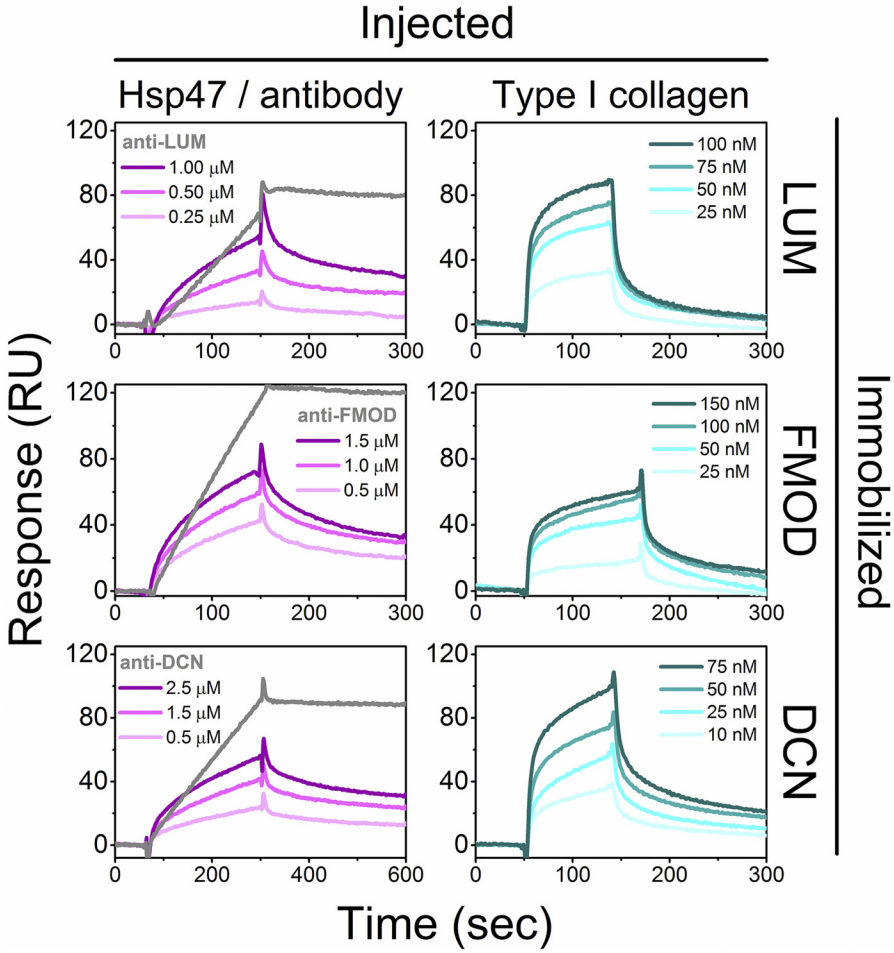

Figure 3. Determination of the direct interaction between SLRPs and Hsp47 or type I collagen. Direct binding kinetics were measured by SPR analysis using a BIAcore X instrument. Various concentrations of Hsp47 and type I collagen were run over the LUM, fibromodulin (*FMOD*), and DCN chip. An antibody was used as a positive control. All curves are the average of at least three replicates of three independent measurements.

rER. These results also suggest that Hsp47 binds nonglycosylated SLRPs because substitution of the SLRPs with glycosaminoglycans occurs downstream of rER (36).

Surface plasmon resonance analyses of SLRP–Hsp47 interaction

To assess whether Hsp47 directly interacts with SLRPs, surface plasmon resonance (SPR) was performed using lumican, fibromodulin, and decorin immobilized to a chip. Fig. S2 shows the proteins used for the SPR experiments. Injected Hsp47 clearly interacted with all three SLRPs and also showed a concentration-dependent binding (Fig. 3). To compare the binding of SLRPs to Hsp47 *versus* type I collagen, type I collagen was also injected into the SLRP chips, resulting in a concentration-dependent binding (Fig. 3). Next, equilibrium dissociation constants (K_d) were calculated from the binding kinetics (k_a and k_d). Similar K_d values were obtained for Hsp47 interacting with the three different SLRPs. Similar K_d values were also obtained for type I collagen interacting with the three different SLRPs. The SLRPs did, however, interact stronger with collagen than with Hsp47, but the Hsp47–SLRP interactions were still comparable with the Hsp47–collagen interactions (Fig. S3 and Table 1).

Potential complex formation between Hsp47, type I collagen, and SLRPs

To test a potential complex formation between SLRPs, Hsp47, and type I collagen, we performed further SPR analyses with Hsp47, type I collagen, or mixtures of the two that were injected over immobilized lumican, fibromodulin, or decorin. In a previous SPR study on complex formations between Hsp47, type I collagen, and TANGO1 or FKBP65, we found that mixtures of two of the reactants gave higher signals than the sum of signals obtained from injecting each of the proteins alone (16, 37). This implies that the injected reactants associate and form trimeric complexes, thereby yielding a higher signal. The *red curves* in Fig. 4 show Hsp47 and type I collagen co-injected over the SLRPs. Interestingly, these *red curves* always showed lower signals than the *blue curves*, which show the calculated sum of the individual binding signals obtained after injection of Hsp47 or type I collagen alone. This indicates that the three proteins do not form a trimeric complex but that Hsp47 and SLRPs compete to interact with type I collagen (16, 37).

This difference was most prominent in experiments with decorin, whose strong binding to collagen was reduced in the presence of Hsp47. For lumican and fibromodulin, similar

Table 1

The binding affinities between Hsp47, SLRPs, and collagens

The results are shown as mean ± S.D., calculated from three independent measurements. Data were calculated by a global fit of the concentration-dependent measurements using the Langmuir model.

Immobilized	Injected	k_a	k_d	K_d	*p* value for K_d
		$10^4\ M^{-1}\ s^{-1}$	$10^{-3}\ s^{-1}$	$10^{-7}\ M$	
Lumican	Hsp47	0.397 ± 0.155	6.23 ± 0.84	16.9 ± 5.0	0.0012
	Type I collagen[a]	26.3 ± 6.87	22.9 ± 4.92	0.88 ± 0.07	
Fibromodulin	Hsp47	0.796 ± 0.389	4.03 ± 1.91	5.9 ± 3.9	0.0292
	Type I collagen[a]	11.6 ± 0.99	12.4 ± 0.38	1.07 ± 0.09	
Decorin	Hsp47	0.371 ± 0.005	2.15 ± 0.25	5.8 ± 0.7	0.000012
	Type I collagen[a]	35.3 ± 1.00	7.35 ± 0.23	0.22 ± 0.06	
Type I collagen[a]	Hsp47	6.12 ± 0.64	23.5 ± 0.60	3.87 ± 0.49	

[a] Type I collagen was treated with pepsin.

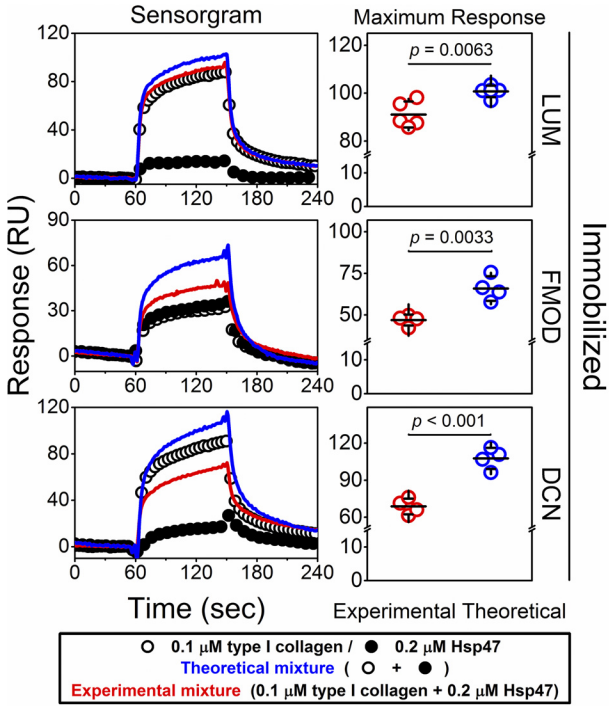

Figure 4. Comprehensive binding analysis between SLRPs, Hsp47, and type I collagen. SPR analysis was carried out using a BIAcore X instrument to characterize the binding manner of type I collagen and Hsp47 to the SLRP chips. *Open* and *closed circles*, type I collagen (0.1 μM) and Hsp47 (0.2 μM), respectively. *Blue curves*, theoretical signal derived from the addition of individual type I collagen and Hsp47 curves. *Red curves*, experimental data from co-injected mixture of type I collagen and s47. The *left panels* display live sensorgrams, and the *right panels* indicate the maximum responses determined by the values just before the dissociation starts, excluding the sharp noise caused by stopping the injection. *Black lines*, mean ± S.D. (*error bars*). All curves are the average of at least three replicates of three independent measurements.

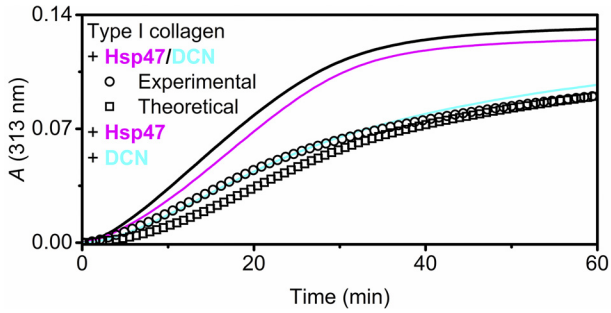

Figure 5. Influence of Hsp47 and decorin on *in vitro* fibril formation of type I collagen. A stock solution of type I collagen in 50 mM acetic acid was diluted to a final concentration of 0.1 μM. Fibril formation in the absence (*black*) and presence of 0.1 μM Hsp47 (*magenta*) and 0.05 μM DCN (*cyan*) was monitored as absorbance at 313 nm. The *squares* and *circles* indicate the theoretical signal derived from the addition of individual Hsp47 and decorin signals and the experimental signal from a mixture of Hsp47 and decorin, respectively. All curves are the average of at least three independent measurements.

interaction inhibition by Hsp47 was observed, although to a lesser extent (Fig. 4).

To further investigate the interactions between collagen, Hsp47, and decorin, an established *in vitro* collagen fibril formation assay was used. This assay monitors inhibition of collagen fibrillogenesis over time as a function of interaction between collagen and other proteins or molecules (37, 38). Collagen fibrillogenesis was delayed slightly by Hsp47 but more efficiently by decorin or by a mixture of Hsp47 and decorin (Fig. 5). Comparison of the decorin curve with the mixture curve shows intriguing, statistically significant differences at the beginning (≤9 min) and at the end (45–60 min) of the measurement (see Table 2 for detailed analysis). Furthermore, the experimental mixture curve was also compared with a theoretically calculated curve, the latter derived by adding the experimental curves of Hsp47 and decorin alone. This comparison revealed less inhibitory effect from the experimental than from the theoretical curve until around 40 min and then no significant differences from that point to the end of the measurement (Fig. 5). The mode of binding between these three molecules is initially competitive when mostly small type I collagen aggregates are present. It then transitions into cooperative binding for larger collagen fibrils.

Investigation of SLRPs' interactions with the SH3 domain of TANGO1 (the procollagen-associated sorting protein at ER exit sites)

During synthesis of type I collagen, Hsp47 anchors newly synthesized collagen molecules to the rER protein TANGO1 (16, 37). TANGO1 that is localized at ER exit sites plays an important role in collagen secretion by enabling the formation of secretory vesicles for procollagen (10, 39). In a recent study, Hsp47 was identified as an anchor protein for the sorting of collagen, as Hsp47 was observed to be bind TANGO1 through an interaction with the SH3 domain of TANGO1 (16). Therefore, we hypothesized that Hsp47 could also sort SLRPs to be loaded into the same COPII vesicles as collagens. SPR was performed to investigate potential interactions between SLRPs, Hsp47, and the SH3 domain of TANGO1. Fig. 6 shows that the

Table 2

Absorbance ($A_{313\ nm}$) signal differences measured in the *in vitro* collagen fibril formation assay

The results are shown as mean ± S.D., obtained from three independent measurements. The graphs are shown in Fig. 5. The competitive binding state occurs when $A_{(experimental)} > A_{(DCN)} > A_{(theoretical)}$. The intermediate binding state occurs when $A_{(experimental)} \approx A_{(DCN)} > A_{(theoretical)}$. The cooperative binding state occurs when $A_{(DCN)} > A_{(experimental)} \approx A_{(theoretical)}$.

Time	DCN	DCN + Hsp47 (experimental)	*p* value (DCN *versus* experimental)	DCN + Hsp47 (theoretical)	*p* value (experimental *versus* theoretical)
min					
3	0.00275 ± 0.000085	0.00388 ± 0.000327	0.0044	0.00105 ± 0.000637	0.0024
6	0.00704 ± 0.000261	0.00844 ± 0.000536	0.0154	0.00331 ± 0.000945	0.0012
9	0.0143 ± 0.00049	0.0157 ± 0.00075	0.0442	0.0078 ± 0.00131	0.0008
12	0.0225 ± 0.00071	0.0240 ± 0.00097	0.1016	0.0138 ± 0.00142	0.0004
15	0.0311 ± 0.00106	0.0326 ± 0.00121	0.1782	0.0211 ± 0.00166	0.0006
20	0.0435 ± 0.00151	0.0447 ± 0.00129	0.3265	0.0331 ± 0.00198	0.0010
25	0.0561 ± 0.00176	0.0562 ± 0.0012	0.9627	0.0469 ± 0.00183	0.0018
30	0.0651 ± 0.00195	0.0638 ± 0.00105	0.3748	0.0573 ± 0.00160	0.0039
35	0.0725 ± 0.00225	0.0701 ± 0.00088	0.1525	0.0655 ± 0.00186	0.0154
40	0.0796 ± 0.00241	0.0760 ± 0.00076	0.0676	0.0726 ± 0.00184	0.0427
45	0.0847 ± 0.00260	0.0802 ± 0.00068	0.0444	0.0777 ± 0.00199	0.1024
50	0.0892 ± 0.00267	0.0839 ± 0.00062	0.0290	0.0822 ± 0.00206	0.2417
55	0.0937 ± 0.00272	0.0876 ± 0.00059	0.0192	0.0867 ± 0.00209	0.4599
60	0.0971 ± 0.00273	0.0904 ± 0.00055	0.0139	0.0899 ± 0.00203	0.7299

SH3 domain of TANGO1 barely binds to SLRPs even at a 10-fold higher molarity than Hsp47. Furthermore, the binding of Hsp47 to fibromodulin was slightly inhibited, and the binding of Hsp47 to lumican and decorin was not significantly affected by the simultaneous presence of the SH3 domain of TANGO1. By comparing the *red experimental curves* in Fig. 6 with the curves constructed by adding the signals yielded after injection of each reactant alone (*blue curves* in Fig. 6), we concluded that SLRPs, Hsp47, and the TANGO1 SH3 domain do not form complexes.

Effects of Hsp47 knockdown on secretion of SLRPs

To assess the functional effect of Hsp47 binding to SLRPs, fibroblast cultures (NIH/3T3 cell line) were used to knock down Hsp47 expression using shRNA. The knockdown of Hsp47 was confirmed by immunoblotting and resulted in stalled secretion of decorin and lumican as well as of collagen, whereas the intracellular levels of protein-disulfide isomerase, calreticulin, and β-actin were unchanged (Fig. 7*A*). As a note, fibromodulin was not detectable in the medium from both control and knockdown samples, probably due to low cellular synthesis of this protein. In these experiments, the intracellular fractions were assayed for the presence of accumulated decorin and lumican, but both proteins were detected neither by immunoblots (in Nonidet P-40– or in radioimmune precipitation assay buffer–solubilized cell lysate) nor by immunofluorescence microscopy (data not shown). In other words, the low endogenous expression of SLRPs allowed the detection of lumican and decorin only in the concentrated secreted fractions.

The Hsp47 knockdown did not significantly change total protein secretion, except for some proteins; this was indicated by the [^{35}S]methionine/cysteine-labeled protein secretion rates that were similar in knockdown and in negative control samples (Fig. 7*B*). Also, apoptosis, assessed by measuring hexosaminidase release (data not shown), was detected neither in Hsp47 nor in control knockdown cultures.

Last, to assess the Hsp47 knockdown effect on SLRP and collagen mRNA levels, quantitative PCR assays were performed on the transfected cells. None of the investigated transcripts showed significant changes (Table 3).

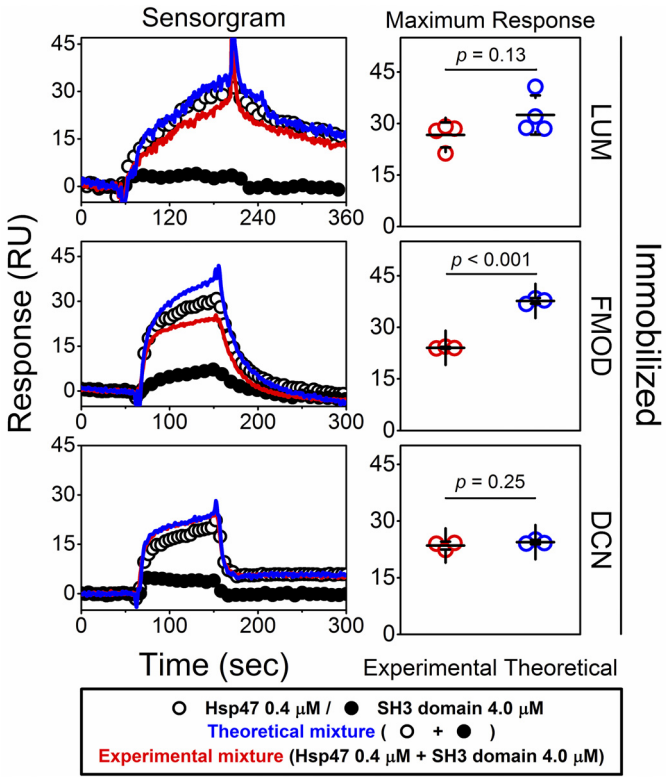

Figure 6. Comprehensive binding analysis between SLRPs, Hsp47, and the SH3 domain of TANGO1. SPR analysis was carried out using a BIAcore X instrument to characterize the binding manner of Hsp47 and the SH3 domain of TANGO1 to the SLRP chips. *Open* and *closed circles*, Hsp47 (0.4 μM) and the SH3 domain of TANGO1 (4.0 μM), respectively. *Blue curves*, theoretical signal derived from the addition of individual Hsp47 and the SH3 domain of TANGO1 curves. *Red curves*, experimental data from co-injected mixture of Hsp47 and the SH3 domain of TANGO1. The *left panels* show live sensorgrams, and the *right panels* indicate maximum responses determined by the values right before starting the dissociation process, excluding the sharp noise caused by stopping the injection. *Black lines*, mean ± S.D. (*error bars*). All curves are the average of at least three replicates of three independent measurements.

Discussion

In this study, we found that three SLRPs, lumican, decorin, and fibromodulin, directly interact with the ER-resident Hsp47, at affinities comparable with Hsp47–collagen interactions (Table 1). However, SLRPs, unlike FKBP65 and TANGO1, pre-

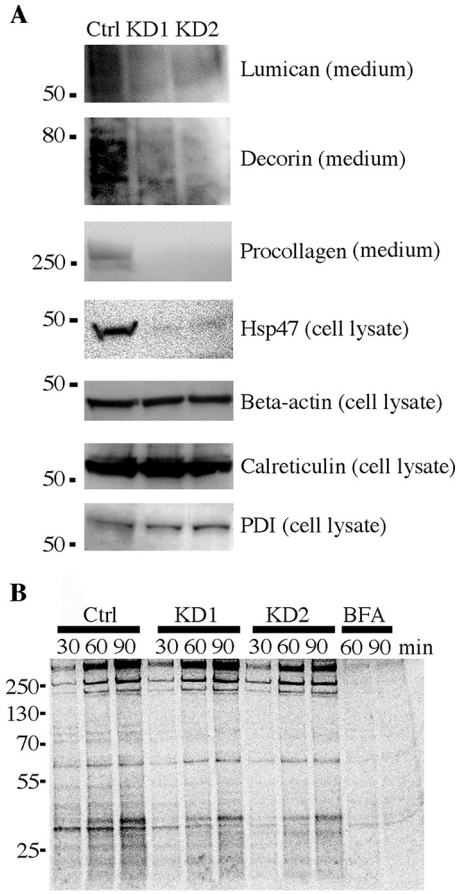

Figure 7. Knockdown of Hsp47 stalls SLRP secretion. *A*, Hsp47 knockdown in NIH/3T3 cells. Cells were transfected with negative control shRNA (*Ctrl*) or with Hsp47 shRNA (two constructs, KD1 and KD2). Concentrated cell medium collected for 24 h at days 2–3 post-transfection or cell lysate collected at day 3 post-transfection was run on SDS-PAGE and blotted for the listed proteins. *B*, total protein secretion from NIH/3T3 cells after Hsp47 knockdown (construct KD1 or KD1) or negative control construct (*Ctrl*). Day 2 post-transfection, the cell medium was changed to cysteine/methionine-free DMEM supplemented with ^{35}S protein-labeling mix. Some cells were treated with brefeldin A (*BFA*) as a positive control for stalled secretion. The medium was removed 30, 60, and 90 min after pulse, run on SDS-PAGE, and developed on a radiographic film. *PDI*, protein-disulfide isomerase.

Table 3

Quantitative PCR on NIH/3T3 cells 3 days after transfection with negative control shRNA or Hsp47 knockdown shRNA

The data were generated from three biological replicates for each shRNA. Change represents the percentage change relative to negative controls. *p* values were calculated using Student's unpaired *t* test. Ctrl, control shRNA; KD1 and KD2, Hsp47 knockdown shRNA 1 and 2.

Transcript	Sample	δCt	S.D.	Change	*p*
				%	
Col1a1	Ctrl	−2.2	0.2		
	KD1	−2.2	0.01	−1	0.92
	KD2	−2.2	0.4	0	0.96
Dcn	Ctrl	3.6	0.7		
	KD1	4.3	0.2	−40	0.28
	KD2	3.8	0.3	−15	0.42
Lum	Ctrl	8.3	0.7		
	KD1	8.8	0.2	−30	0.43
	KD2	7.8	0.1	+40	0.44
Fmod	Ctrl	9.6	0.1		
	KD1	9.6	0.1	+2	0.77
	KD2	9.6	0.2	+1	0.91
Serpinh1	Ctrl	2.8	0.03		
	KD1	5.6	0.002	−86	0.000061
	KD2	5.6	0.2	−86	0.0036

sumably do not form a complex with both Hsp47 and type I collagen, as demonstrated by our SPR data (Fig. 4). Hsp47 largely interfered with the binding between decorin and type I collagen and, to a lesser extent, between fibromodulin or lumican and type I collagen. The differences between the three SLRPs' structures (decorin belongs to class I and lumican/fibromodulin belong to class II of SLRPs) or in the theoretical pI (8.61 for decorin and 6.17/5.66 for lumican/fibromodulin) could explain why the larger effect on decorin–collagen interaction was observed in the presence of Hsp47.

Moreover, Hsp47 also affected type I collagen fibril formation in the presence of decorin (Fig. 5 and Table 2), notably at the beginning and at the end of fibrillogenesis. The initial effect results probably from competitive binding, suggested from the SPR results in Fig. 4, whereas a cooperative binding is suggested from the overlapping experimental and theoretical curves at the end of the measurement. We suggest that these effects reflect the altering binding affinities of Hsp47 and decorin for collagen monomers/initial thin fibrils *versus* the later-forming thicker fibrils. Also, new binding sites may occur on growing fibrils.

Furthermore, we validated the functional significance of the SLRP–Hsp47 interactions by knocking down Hsp47 in NIH/3T3 cells and studying its effects on SLRPs. The Hsp47 knockdown stalled the secretion of not only collagen but also of the now-identified interactants lumican and decorin, suggesting that Hsp47 is not only a collagen-specific binding protein but also functions in SLRP secretion.

These results suggest that Hsp47 not only plays a role in collagen folding and secretion (16–18) but also functions in the secretion of SLRPs. In further support of this notion is the absence of Hsp47 knockdown effects on collagen and SLRP transcripts (*i.e.* the stalled secretion of SLRPs cannot be explained by transcriptional down-regulation (*e.g.* due to off-target effects from shRNA or due to negative feedback on transcription)). Also, general protein secretion after Hsp47 knockdown appears largely unaffected, except for some proteins, which may be secondary to protein aggregation in the ER, as reported previously (17, 40), or due to Hsp47 modulating the secretion of other, yet unknown, proteins. Regardless of this, our data still point to a function of Hsp47 in the secretion of procollagen and SLRPs. We did, however, observe that the secretion of SLRPs, unlike that of procollagen, does not involve the previously described complex formation between Hsp47 and the SH3 domain of TANGO1 (1, 10, 16, 37).

To summarize, it was previously shown that Hsp47 plays a central role in the quality control of collagen folding and secretion. It probably acts as a hub molecule by enabling FKBP65 and TANGO1 to interact with collagens during collagen folding and secretion (37). Here, we propose a novel function of Hsp47. Hsp47 directly interacts with the SLRPs lumican, decorin, and fibromodulin and may temporally prevent SLRPs from binding to collagen molecules in the rER, which in turn would prevent the formation of large ECM complexes inside the cells. This would indirectly ensure a proper secretion of procollagen by the TANGO1 pathway and also the secretion of SLRPs. We also suggest that large macromolecular aggregates may be formed by collagen fibrils, SLRPs, and possibly other ECM ligands if

Hsp47 fails to prevent an excessive association between collagen molecules. Further studies are required to identify the binding sites between Hsp47 and SLRPs and how collagens are isolated from other collagen-interacting ECM molecules, such as integrins and fibronectin.

Experimental procedures

Recombinant proteins

His-tagged recombinant decorin, fibromodulin, and lumican were expressed in 293 cells, as described previously (42–44). The proteins were purified on Ni^{2+}-nitrilotriacetic acid columns (Qiagen) and desalted on a Superose 6 column using Äkta chromatography equipment (GE Healthcare). His-tagged Hsp47 was expressed in Xj(b) *E. coli* cells (Zymoresearch) using pET-27(b) vector (Novagen) and purified in native PBS buffer according to the Qiaexpressionist protocol (Qiagen) and dialyzed into PBS. Where needed, proteins were biotinylated using EZ-link NHS-biotin (Thermo Fisher Scientific).

Preparation of endogenous chicken Hsp47, the recombinant SH3 domain of human TANGO1, and mouse type I collagen

Endogenous chicken Hsp47 and the recombinant SH3 domain of human TANGO1 were purified from 17-day-old chicken embryos and *E. coli* by the methods described previously (16, 45). Mouse type I collagen was extracted from tail tendon as described previously (46).

Far-Western blotting

Differentiating chondrocyte-like ATDC5 cells were lysed in cold PBS containing 1% (v/v) Nonidet P-40 and protease inhibitors for 15 min on ice. The lysates were cleared by centrifugation, protein amount was quantified with a BCA assay, and 40 μg of total protein was run on SDS-PAGE and transferred to a nitrocellulose membrane. The membrane was washed for 10 min with TBS; blocked with 5% (w/v) BSA in TBS (blocking buffer) for 4 h; incubated with biotinylated decorin, fibromodulin, lumican, or BSA at 1 μg/ml in blocking buffer overnight at 4 °C; and then washed three times for 10 min each in TBS with 0.05% (v/v) Tween 20 (TBST). Then the membrane was incubated with HRP-conjugated streptavidin diluted 1:50,000 in blocking buffer and incubated for 1 h, washed 3 × 10 min in TBST, and developed using Luminata forte (Millipore) and a CCD camera.

Mass spectrometry

Gel bands were cut out, in-gel–digested with trypsin, and processed for LC-MS/MS MS at a local core facility (Medicon Village, Lund, Sweden).

Co-immunoprecipitation assays

100 μl of clarified lysates from ATDC5 cells (2 mg of total protein) were incubated with 1 μg of His-tagged fibromodulin or lumican and with 1 μg of mouse anti-His antibody (Abcam 18184) overnight at 4 °C in TBS with 1% (v/v) Nonidet P-40 (lysis buffer). As a negative control, we incubated lysates without the His-tagged proteins but with an anti-His antibody. Another assay was performed using a combination of 1 μg of recombinant decorin and 5 μl of decorin antiserum (kind gift from Prof. Åke Oldberg, Lund University). Then 40 μl of Protein G– or Protein A–Sepharose (Thermo Fisher Scientific), to capture anti-His and anti-decorin, respectively, were added and incubated with gentle rotation for 2 h at room temperature. The beads were washed twice with lysis buffer and then twice with PBS, and then the proteins were eluted with 1% (w/v) SDS, separated on SDS-PAGE, and transferred to a nitrocellulose membrane. Immunoblots for Hsp47 were performed by blocking the membrane in 5% (w/v) BSA in TBS for 1 h and then incubating with anti-Hsp47 (Abcam 109117) diluted 1:1,000 in 5% (w/v) BSA in TBST, washing three times for 5 min each with TBST, incubating with HRP-conjugated Protein A (Abcam) diluted 1:5,000 in 5% (w/v) BSA in TBST, washing three times for 5 min each in TBST, and developing the membrane using Luminata Forte (Millipore).

Pulldown assays

Recombinant Hsp47 or BSA was covalently coupled to magnetic beads using Dynabeads according to the manufacturer's instructions (Thermo Fisher Scientific) and blocked with 1% (w/v) BSA. The beads were incubated with biotinylated decorin, lumican, or fibromodulin diluted to 1 μg/ml in 1% (w/v) BSA in TBS, for 1 h, rotating at room temperature, and then washed four times with TBST and eluted with 1% (w/v) SDS. Eluates were run on SDS-PAGE, transferred to a nitrocellulose membrane, and immunoblotted for decorin, lumican, or fibromodulin using streptavidin-HRP, using the same procedure as in far-Western blotting (described above).

Proximity ligation assays (PLAs)

PLAs were used here to detect intracellular protein–protein interactions. In general, this method detects the presence of two antibodies (against the proteins of interest) that bind in the proximity of <40 nm of each other. To detect the interactions, two primary antibodies raised in different species are incubated with the samples. The samples are then incubated with secondary antibodies conjugated with unique DNA probes that, if the antibodies are in close proximity and in the presence of additional substrates and enzymes, will be used for rolling circle DNA synthesis that results in multifold amplification of the DNA. The amplified DNA is then detected by complementary fluorescence-labeled oligonucleotides (41).

To detect Hsp47–SLRP interactions, we used BJ cells (human foreskin fibroblast cell line) grown in DMEM with 10% (v/v) FBS and transfected with shRNAs: Silencer® Select *SERPINH1* probe (for Hsp47 knockdown) or universal negative control probe (both from Thermo Fisher Scientific), at 10 nM, using RNAiMAX reagent according to the manufacturer's instructions (Thermo Fisher Scientific). After 2 days, the cells were trypsinized and seeded onto 8-well chamber glass slides and grown for an additional 2 days in DMEM supplemented with 50 μg/ml ascorbate. A portion of the cells was lysed in PBS with 1% Nonidet P-40 and protease inhibitor mixture (Roche Applied Science) and used to confirm the Hsp47 knockdown by immunoblotting, using protocols described for co-immunoprecipitation assays. The cells were washed three times with PBS, fixed in 4% paraformaldehyde in PBS for 10 min, washed

with 0.1 M glycine in PBS for 10 min, and then washed three times with PBS for 5 min (all solutions were ice-cold and buffered to pH 7.4). The PBS was briefly centrifuged off the glass slides, and the slides were air-dried and stored at −20 °C until later use.

For the PLAs, the slides were thawed on ice, covered with PBS for 10 min, and then permeabilized with PBS + 0.5% Triton X-100 for 5 min at room temperature and washed with PBS three times for 5 min each. Duolink PLAs (Sigma) were performed with solutions provided by the manufacturer, unless stated otherwise. The cell slides were blocked with Duolink blocking solution for 1 h at 37 °C. Primary antibodies or antisera were diluted in Duolink antibody dilution buffer and incubated on the slides overnight at 4 °C. Here, Hsp47 was detected with mouse anti-Hsp47 (Abcam 86750) diluted 1:250 or rabbit anti-Hsp47 (Abcam 109117) diluted 1:1,000, whereas lumican or decorin were detected with anti-lumican (in-house antiserum, validated on lumican knockout tissue; see Fig. S4) or with anti-decorin (kind gift from Prof. Åke Oldberg), both diluted 1:700. After the primary antibody incubation, the cell slides were washed three times for 5 min each with TBS, pH 7.4, with 0.05% Tween 20 (TBST, in-house) and incubated with Duolink anti-mouse PLUS and Duolink anti-rabbit MINUS probes diluted 1:5 in Duolink antibody dilution buffer and incubated on samples for 1 h at 37 °C. For negative controls, both secondary antibodies were used but with one primary antibody (all four primary antibodies were tested separately in this setting). After three 5-min washes with TBST, the slides were incubated with T4 ligase diluted 1:40 into Duolink ligation buffer, for 30 min at 37 °C, and then washed three times for 5 min each with TBST. Then the slides were incubated with Phi29 polymerase diluted 1:80 into Duolink Amplification Buffer Red 1×, for 100 min at 37 °C and washed three times for 10 min each with TBST. Finally, the slides were counterstained for F-actin and nuclei with Phalloidin-Alexa Fluor 488 diluted 1:40 into Hoechst solution (Thermo Fisher Scientific), for 15 min at room temperature. The slides were then rinsed with water and mounted using SlowFade mounting medium (Thermo Fisher Scientific).

SPR analysis

SPR experiments were carried out using a BIAcore X instrument (GE Healthcare). Three purified SLRPs (lumican, fibromodulin, and decorin) or type I collagen was immobilized on CM5 sensor chips by amide coupling. The approximate coupled protein concentrations were 3.5 ng/mm^2 (3,500 response units (RU)) of lumican, 4.8 ng/mm^2 (4,800 RU) of fibromodulin, 1.5 ng/mm^2 (1,500 RU) of decorin, and 3.2 ng/mm^2 (3,200 RU) of type I collagen. To prevent analytes from binding to the dextran nonspecifically, RNase A was used as a ligand for a reference channel to mask the dextran surface. The experiments were performed at 20 °C in HBS-P buffer (10 mM Hepes buffer, pH 7.4, 150 mM NaCl, and 0.005% (v/v) Surfactant P20) containing 1 mM $CaCl_2$. Individual binding curves for type I collagen, Hsp47, and the SH3 domain of TANGO 1 were obtained by injecting these proteins onto immobilized SLRPs. For comprehensive binding analysis between SLRPs and Hsp47 in the presence of either type I collagen or the SH3 domain of TANGO1, the mixtures of Hsp47 + type I collagen or Hsp47 + SH3 domain of TANGO1 were injected onto immobilized SLRPs (the mixtures were prepared just before the injection). Experimentally obtained binding curves of mixtures were compared with theoretical signals derived from the addition of individual experimental binding curves of Hsp47, type I collagen, or the SH3 domain of TANGO1. A control experiment is shown in Fig. S5, validating the additivity of binding curves where no interaction exists between two ligands. For analysis of binding affinity, the curves were fitted with the Langmuir binding model (BIAevaluation software; GE Healthcare). All curves are the average of at least three independent measurements.

Type I collagen fibril formation assay

Fibril formation assays of type I collagen were measured at 34 °C in a Cary 4 series UV-visible spectrophotometer (Agilent Technologies), and the absorbance (light scattering) was monitored at 313 nm as a function of time. Stock solutions of type I collagen in 50 mM acetic acid were diluted to a final concentration of 0.1 μM in 0.1 M sodium phosphate buffer, pH 7.8, containing 0.15 M NaCl (assay buffer). Collagen solutions were then added to assay buffers supplemented with Hsp47, decorin, or a mixture of Hsp47 and decorin. A control solution containing only collagen in assay buffer was also run. Experimentally obtained curves of Hsp47 + decorin mixtures were compared with the theoretical signals derived from the addition of individual experimental curves of Hsp47 and decorin. All curves are the average of at least three independent measurements.

Cell culture Hsp47 knockdown experiments

NIH/3T3 cells were grown in DMEM with 10% (v/v) FBS to subconfluence, the medium was supplemented with 50 μg/ml ascorbate, and the cells were transfected with Silencer® Select *Serpinh1* probes (s232335 and s63466) or universal negative control probe (all from Thermo Fisher Scientific) at 10 nM using RNAiMAX reagent, according to the manufacturer's instructions (Thermo Fisher Scientific). After 2 days, the cells were washed three times with PBS and changed to serum-free DMEM supplemented with 50 μg/ml ascorbate. The medium was collected the following day, and the proteins were acetone-precipitated. In parallel, 1% (v/v) Nonidet P-40 and radioimmune precipitation assay buffer lysates were collected from transfected cells grown in DMEM with 10% (v/v) FBS. Proteins were fractionated on a 4–12% BisTris SDS-PAGE (Thermo Fisher Scientific), transferred to a nitrocellulose membrane, and immunoblotted using antibodies against β-actin (Abcam 6276), Hsp47 (Abcam 109117), lumican (in-house–made antiserum), decorin (gift from Prof. Åke Oldberg), procollagen type I (LF-39 antiserum, kind gift from Dr. Larry W. Fisher, National Institutes of Health), calreticulin (Abcam 14234, now discontinued), or protein-disulfide isomerase (Abcam RL77). Immunoblots were performed as described above (see "Co-immunoprecipitation assays").

For [^{35}S]methionine/cysteine labeling, the cells were treated as above, but 2 days post-transfection, the medium was exchanged to cysteine- and methionine-free DMEM (Sigma), and supplemented with 50 μCi/ml ^{35}S EasyTag Express Protein Labeling Mix (PerkinElmer Life Sciences). A stalled secretion positive

control sample was included where cells were supplemented with 10 μg/ml brefeldin A 15 min before the labeling and then throughout the labeling process. The medium was removed after 30, 60, and 90 min and run on SDS-polyacrylamide gels that were then dried and developed using FujiFilm.

Reverse transcription and RT-PCR

Cells used in the knockdown experiments were lysed in TRIzol reagent 3 days post-transfection (Thermo Fisher Scientific), and RNA was isolated and used in a reverse transcription reaction using SuperScript VILO (Thermo Fisher Scientific). RT-PCR with Taqman probes (Thermo Fisher Scientific) was performed on an Applied Biosystems 7300 detection system.

Statistical analyses

For comparisons between two groups, we performed one-way analysis of variance to determine whether differences between groups are significant. ORIGIN Pro version 9.1 was used. A p value < 0.05 was considered statistically significant.

Author contributions—Y. I., K. R., H. P. B., and S. K. conceptualization; Y. I., K. R., H. P. B., and S. K. resources; Y. I., K. R., H. P. B., and S. K. data curation; Y. I., K. R., H. P. B., and S. K. formal analysis; Y. I., K. R., H. P. B., and S. K. funding acquisition; Y. I., K. R., H. P. B., and S. K. validation; Y. I., K. R., and S. K. investigation; Y. I., K. R., H. P. B., and S. K. methodology; Y. I., K. R., H. P. B., and S. K. writing-original draft; Y. I. and S. K. project administration; H. P. B. and S. K. supervision.

Acknowledgment—In situ PLA was performed by the PLA Proteomics Facility (Uppsala, Sweden), which is supported by Science for Life Laboratory (Solna, Sweden).

References

1. Malhotra, V., and Erlmann, P. (2015) The pathway of collagen secretion. *Annu. Rev. Cell Dev. Biol.* **31,** 109–124 CrossRef Medline
2. Gomez-Navarro, N., and Miller, E. (2016) Protein sorting at the ER-Golgi interface. *J. Cell Biol.* **215,** 769–778 Medline
3. Gorur, A., Yuan, L., Kenny, S. J., Baba, S., Xu, K., and Schekman, R. (2017) COPII-coated membranes function as transport carriers of intracellular procollagen I. *J. Cell Biol.* **216,** 1745–1759 CrossRef Medline
4. Canty-Laird, E. G., Lu, Y., and Kadler, K. E. (2012) Stepwise proteolytic activation of type I procollagen to collagen within the secretory pathway of tendon fibroblasts in situ. *Biochem. J.* **441,** 707–717 CrossRef Medline
5. Humphries, S. M., Lu, Y., Canty, E. G., and Kadler, K. E. (2008) Active negative control of collagen fibrillogenesis *in vivo*: intracellular cleavage of the type I procollagen propeptides in tendon fibroblasts without intracellular fibrils. *J. Biol. Chem.* **283,** 12129–12135 CrossRef Medline
6. Eyre, D. R., and Weis, M. A. (2013) Bone collagen: new clues to its mineralization mechanism from recessive osteogenesis imperfecta. *Calcif. Tissue Int.* **93,** 338–347 CrossRef Medline
7. Marini, J. C., and Blissett, A. R. (2013) New genes in bone development: what's new in osteogenesis imperfecta. *J. Clin. Endocrinol. Metab.* **98,** 3095–3103 CrossRef Medline
8. Ishikawa, Y., and Bächinger, H. P. (2013) A molecular ensemble in the rER for procollagen maturation. *Biochim. Biophys. Acta* **1833,** 2479–2491 CrossRef Medline
9. Wilson, D. G., Phamluong, K., Li, L., Sun, M., Cao, T. C., Liu, P. S., Modrusan, Z., Sandoval, W. N., Rangell, L., Carano, R. A., Peterson, A. S., and Solloway, M. J. (2011) Global defects in collagen secretion in a Mia3/TANGO1 knockout mouse. *J. Cell Biol.* **193,** 935–951 CrossRef Medline
10. Saito, K., Chen, M., Bard, F., Chen, S., Zhou, H., Woodley, D., Polischuk, R., Schekman, R., and Malhotra, V. (2009) TANGO1 facilitates cargo loading at endoplasmic reticulum exit sites. *Cell* **136,** 891–902 CrossRef Medline
11. Ma, W., and Goldberg, J. (2016) TANGO1/cTAGE5 receptor as a polyvalent template for assembly of large COPII coats. *Proc. Natl. Acad. Sci. U.S.A.* **113,** 10061–10066 CrossRef Medline
12. Tanabe, T., Maeda, M., Saito, K., and Katada, T. (2016) Dual function of cTAGE5 in collagen export from the endoplasmic reticulum. *Mol. Biol. Cell* **27,** 2008–2013 CrossRef Medline
13. Venditti, R., Scanu, T., Santoro, M., Di Tullio, G., Spaar, A., Gaibisso, R., Beznoussenko, G. V., Mironov, A. A., Mironov, A., Jr., Zelante, L., Piemontese, M. R., Notarangelo, A., Malhotra, V., Vertel, B. M., Wilson, C., and De Matteis, M. A. (2012) Sedlin controls the ER export of procollagen by regulating the Sar1 cycle. *Science* **337,** 1668–1672 CrossRef Medline
14. Maeda, M., Katada, T., and Saito, K. (2017) TANGO1 recruits Sec16 to coordinately organize ER exit sites for efficient secretion. *J. Cell Biol.* **216,** 1731–1743 CrossRef Medline
15. Schmidt, K., Cavodeassi, F., Feng, Y., and Stephens, D. J. (2013) Early stages of retinal development depend on Sec13 function. *Biol. Open* **2,** 256–266 CrossRef Medline
16. Ishikawa, Y., Ito, S., Nagata, K., Sakai, L. Y., and Bächinger, H. P. (2016) Intracellular mechanisms of molecular recognition and sorting for transport of large extracellular matrix molecules. *Proc. Natl. Acad. Sci. U.S.A.* **113,** E6036–E6044 CrossRef Medline
17. Ishida, Y., Kubota, H., Yamamoto, A., Kitamura, A., Bächinger, H. P., and Nagata, K. (2006) Type I collagen in Hsp47-null cells is aggregated in endoplasmic reticulum and deficient in N-propeptide processing and fibrillogenesis. *Mol. Biol. Cell* **17,** 2346–2355 CrossRef Medline
18. Nagai, N., Hosokawa, M., Itohara, S., Adachi, E., Matsushita, T., Hosokawa, N., and Nagata, K. (2000) Embryonic lethality of molecular chaperone hsp47 knockout mice is associated with defects in collagen biosynthesis. *J. Cell Biol.* **150,** 1499–1506 CrossRef Medline
19. Matsuoka, Y., Kubota, H., Adachi, E., Nagai, N., Marutani, T., Hosokawa, N., and Nagata, K. (2004) Insufficient folding of type IV collagen and formation of abnormal basement membrane-like structure in embryoid bodies derived from Hsp47-null embryonic stem cells. *Mol. Biol. Cell* **15,** 4467–4475 CrossRef Medline
20. Christiansen, H. E., Schwarze, U., Pyott, S. M., AlSwaid, A., Al Balwi, M., Alrasheed, S., Pepin, M. G., Weis, M. A., Eyre, D. R., and Byers, P. H. (2010) Homozygosity for a missense mutation in SERPINH1, which encodes the collagen chaperone protein HSP47, results in severe recessive osteogenesis imperfecta. *Am. J. Hum. Genet.* **86,** 389–398 CrossRef Medline
21. Drögemüller, C., Becker, D., Brunner, A., Haase, B., Kircher, P., Seeliger, F., Fehr, M., Baumann, U., Lindblad-Toh, K., and Leeb, T. (2009) A missense mutation in the SERPINH1 gene in Dachshunds with osteogenesis imperfecta. *PLoS Genet.* **5,** e1000579 CrossRef Medline
22. Nakai, A., Satoh, M., Hirayoshi, K., and Nagata, K. (1992) Involvement of the stress protein HSP47 in procollagen processing in the endoplasmic reticulum. *J. Cell Biol.* **117,** 903–914 CrossRef Medline
23. Hirayoshi, K., Kudo, H., Takechi, H., Nakai, A., Iwamatsu, A., Yamada, K. M., and Nagata, K. (1991) HSP47: a tissue-specific, transformation-sensitive, collagen-binding heat shock protein of chicken embryo fibroblasts. *Mol. Cell. Biol.* **11,** 4036–4044 CrossRef Medline
24. Sepulveda, D., Rojas-Rivera, D., Rodríguez, D. A., Groenendyk, J., Köhler, A., Lebeaupin, C., Ito, S., Urra, H., Carreras-Sureda, A., Hazari, Y., Vasseur-Cognet, M., Ali, M. M. U., Chevet, E., Campos, G., Godoy, P., *et al.* (2018) Interactome screening identifies the ER luminal chaperone Hsp47 as a regulator of the unfolded protein response transducer IRE1α. *Mol. Cell* **69,** 238–252.e7 CrossRef Medline
25. Olsson, P. O., Gustafsson, R., In 't Zandt, R., Friman, T., Maccarana, M., Tykesson, E., Oldberg, Å., Rubin, K., and Kalamajski, S. (2016) The tyrosine kinase inhibitor imatinib augments extracellular fluid exchange and reduces average collagen fibril diameter in experimental carcinoma. *Mol. Cancer Ther.* **15,** 2455–2464 CrossRef Medline
26. Kalamajski, S., Liu, C., Tillgren, V., Rubin, K., Oldberg, Å., Rai, J., Weis, M., and Eyre, D. R. (2014) Increased C-telopeptide cross-linking of tendon

type I collagen in fibromodulin-deficient mice. *J. Biol. Chem.* **289,** 18873–18879 CrossRef Medline
27. Kalamajski, S., and Oldberg, A. (2010) The role of small leucine-rich proteoglycans in collagen fibrillogenesis. *Matrix Biol.* **29,** 248–253 CrossRef Medline
28. Chen, S., and Birk, D. E. (2013) The regulatory roles of small leucine-rich proteoglycans in extracellular matrix assembly. *FEBS J.* **280,** 2120–2137 CrossRef Medline
29. Danielson, K. G., Baribault, H., Holmes, D. F., Graham, H., Kadler, K. E., and Iozzo, R. V. (1997) Targeted disruption of decorin leads to abnormal collagen fibril morphology and skin fragility. *J. Cell Biol.* **136,** 729–743 CrossRef Medline
30. Zhang, G., Ezura, Y., Chervoneva, I., Robinson, P. S., Beason, D. P., Carine, E. T., Soslowsky, L. J., Iozzo, R. V., and Birk, D. E. (2006) Decorin regulates assembly of collagen fibrils and acquisition of biomechanical properties during tendon development. *J. Cell. Biochem.* **98,** 1436–1449 CrossRef Medline
31. Chakravarti, S., Magnuson, T., Lass, J. H., Jepsen, K. J., LaMantia, C., and Carroll, H. (1998) Lumican regulates collagen fibril assembly: skin fragility and corneal opacity in the absence of lumican. *J. Cell Biol.* **141,** 1277–1286 CrossRef Medline
32. Chakravarti, S., Petroll, W. M., Hassell, J. R., Jester, J. V., Lass, J. H., Paul, J., and Birk, D. E. (2000) Corneal opacity in lumican-null mice: defects in collagen fibril structure and packing in the posterior stroma. *Invest. Ophthalmol. Vis. Sci.* **41,** 3365–3373 Medline
33. Jepsen, K. J., Wu, F., Peragallo, J. H., Paul, J., Roberts, L., Ezura, Y., Oldberg, A., Birk, D. E., and Chakravarti, S. (2002) A syndrome of joint laxity and impaired tendon integrity in lumican- and fibromodulin-deficient mice. *J. Biol. Chem.* **277,** 35532–35540 CrossRef Medline
34. Svensson, L., Aszódi, A., Reinholt, F. P., Fässler, R., Heinegård, D., and Oldberg, A. (1999) Fibromodulin-null mice have abnormal collagen fibrils, tissue organization, and altered lumican deposition in tendon. *J. Biol. Chem.* **274,** 9636–9647 CrossRef Medline
35. Smith, T., Ferreira, L. R., Hebert, C., Norris, K., and Sauk, J. J. (1995) Hsp47 and cyclophilin B traverse the endoplasmic reticulum with procollagen into pre-Golgi intermediate vesicles: a role for Hsp47 and cyclophilin B in the export of procollagen from the endoplasmic reticulum. *J. Biol. Chem.* **270,** 18323–18328 CrossRef Medline
36. Jönsson, M., Eklund, E., Fransson, L. A., and Oldberg, A. (2003) Initiation of the decorin glycosaminoglycan chain in the endoplasmic reticulum-Golgi intermediate compartment. *J. Biol. Chem.* **278,** 21415–21420 CrossRef Medline
37. Ishikawa, Y., Holden, P., and Bächinger, H. P. (2017) Heat shock protein 47 and 65-kDa FK506-binding protein weakly but synergistically interact during collagen folding in the endoplasmic reticulum. *J. Biol. Chem.* **292,** 17216–17224 CrossRef Medline
38. Vogel, K. G., Paulsson, M., and Heinegård, D. (1984) Specific inhibition of type I and type II collagen fibrillogenesis by the small proteoglycan of tendon. *Biochem. J.* **223,** 587–597 CrossRef Medline
39. Liu, M., Feng, Z., Ke, H., Liu, Y., Sun, T., Dai, J., Cui, W., and Pastor-Pareja, J. C. (2017) Tango1 spatially organizes ER exit sites to control ER export. *J. Cell Biol.* **216,** 1035–1049 CrossRef Medline
40. Vranka, J., Mokashi, A., Keene, D. R., Tufa, S., Corson, G., Sussman, M., Horton, W. A., Maddox, K., Sakai, L., and Bächinger, H. P. (2001) Selective intracellular retention of extracellular matrix proteins and chaperones associated with pseudoachondroplasia. *Matrix Biol.* **20,** 439–450 CrossRef Medline
41. Fredriksson, S., Gullberg, M., Jarvius, J., Olsson, C., Pietras, K., Gústafsdóttir, S. M., Ostman, A., and Landegren, U. (2002) Protein detection using proximity-dependent DNA ligation assays. *Nat. Biotechnol.* **20,** 473–477 CrossRef Medline
42. Kalamajski, S., Aspberg, A., and Oldberg, A. (2007) The decorin sequence SYIRIADTNIT binds collagen type I. *J. Biol. Chem.* **282,** 16062–16067 CrossRef Medline
43. Kalamajski, S., Bihan, D., Bonna, A., Rubin, K., and Farndale, R. W. (2016) Fibromodulin interacts with collagen cross-linking sites and activates lysyl oxidase. *J. Biol. Chem.* **291,** 7951–7960 CrossRef Medline
44. Kalamajski, S., and Oldberg, A. (2009) Homologous sequence in lumican and fibromodulin leucine-rich repeat 5–7 competes for collagen binding. *J. Biol. Chem.* **284,** 534–539 CrossRef Medline
45. Macdonald, J. R., and Bächinger, H. P. (2001) HSP47 binds cooperatively to triple helical type I collagen but has little effect on the thermal stability or rate of refolding. *J. Biol. Chem.* **276,** 25399–25403 CrossRef Medline
46. Pokidysheva, E., Zientek, K. D., Ishikawa, Y., Mizuno, K., Vranka, J. A., Montgomery, N. T., Keene, D. R., Kawaguchi, T., Okuyama, K., and Bächinger, H. P. (2013) Posttranslational modifications in type I collagen from different tissues extracted from wild type and prolyl 3-hydroxylase 1 null mice. *J. Biol. Chem.* **288,** 24742–24752 CrossRef Medline